Desalination and Water Treatment
www.deswater.com
doi: 10.1080/19443994.2015.1079262

57 (2016) 16015–16023
July

Taylor & Francis
Taylor & Francis Group

Microwave-assisted one-pot method for preparation of ZnO/AgI nanocomposites with highly enhanced photocatalytic activity under visible-light irradiation

Shirin Shaker-Agjekandy, Aziz Habibi-Yangjeh*

Faculty of Sciences, Department of Chemistry, University of Mohaghegh Ardabili, P.O. Box 179, Ardabil, Iran, email: shaker@uma.ac.ir (S. Shaker-Agjekandy), Tel. +98 045 33514702; Fax: +98 045 33514701; ahabibi@uma.ac.ir (A. Habibi-Yangjeh)

Received 29 April 2015; Accepted 15 July 2015

ABSTRACT

In the present work, a microwave-assisted one-pot method was applied for preparation of the ZnO/AgI nanocomposites. One-pot, large-scale, and short preparation time are main advantages of this method. Photocatalytic activity of the nanocomposites in degradation of rhodamine B under visible-light irradiation is remarkably depended on mole fraction of AgI and the superior activity was seen for the nanocomposite with 0.342 mol fraction of silver iodide. The degradation rate constant over this nanocomposite is about 10-fold higher than that of the ZnO nanostructures. Photoluminescence spectra confirmed that separation of the charge carriers in the nanocomposites is more intensive than the ZnO nanostructures. Furthermore, it was observed that the microwave irradiation time, calcination temperature, and scavengers of the reactive species have considerable influence on the degradation reaction. More importantly, the photocatalyst retains about 80% of its activity after using for five cycles.

Keywords: ZnO/AgI; Microwave-assisted method; Visible-light-driven; Photocatalyst

1. Introduction

In recent years, searching for suitable visible-light-driven photocatalysts for degradation of organic pollutants, hydrogen production from splitting of water, and reduction of carbon dioxide into renewable chemical fuels is one of the significant strategies to address the worldwide arduous challenges facing the human beings [1–3]. Photocatalytic processes have advantages of low energy consumption and environment-friendly property and they are carried out at ambient temperatures and pressures [1–5]. However, the commonly used photocatalysts have shortcomings such as wide band gap and low quantum efficiency, leading to poor photocatalytic activity under the solar irradiation, which seriously restricts their applications for industrial purposes. Hence, preparation of new photocatalysts with high efficiency under visible-light irradiation has attracted widespread attention in the research community [5–9].

Silver containing narrow band gap semiconductors such as AgBr, AgI, Ag_3PO_4, Ag_2CO_3, and Ag_2CrO_4 have intensive absorption in the visible range, leading to their enhanced photocatalytic activities [8–11]. However, these semiconductors have some drawbacks, restricting their practical applications in

*Corresponding author.

industrial scale. Due to the photocorrosion, these semiconductors have low photostability. Furthermore, not only they are expensive but also recombination of electron–hole pairs takes place with high rate [12]. One effective strategy to overcome these shortcomings is combination of silver containing semiconductors with other low-cost semiconductors. For these reasons, in recent years, intensive efforts have been devoted for combining ZnO with various silver containing semiconductors to prepare different visible-light-driven photocatalysts [1,13–18]. In spite of potential photocatalytic activity of ZnO/AgI nanocomposites under visible-light irradiation, there are only a few reports about preparation and investigation of their photocatalytic activities [19–21]. Furthermore, the preparation methods mainly have high temperatures or long reaction times. More importantly, these methods are suffering from multiple-step procedures. Hence, preparation of AgI/ZnO nanocomposites with one-pot methodology will be highly valuable in the field of photocatalytic processes [22]. In recent years, preparation of different nanomaterials using microwave irradiation method has attracted extensive attention, owing to its advantages of short reaction time, small particle size, narrow particle size distribution, and high purity [23–27]. Under microwave irradiation, the electromagnetic waves interact with dipole moments of the molecules, leading to dielectric heating of the reaction system [28]. The literature review showed that there is not any report about preparation of ZnO/AgI nanocomposites using microwave-irradiation method.

Hence, we successfully prepared ZnO/AgI nanocomposites using a microwave-assisted one-pot methodology, for the first time. Activity of the nanocomposites was evaluated by degradation of rhodamine B (RhB) under visible-light irradiation supplied by an LED lamp. Compared to the ZnO nanostructures, a remarkably enhanced photocatalytic activity was observed for the nanocomposites. Furthermore, the effect of silver iodide content, microwave irradiation time, calcination temperature, and scavenger of the reactive species on the degradation reaction was investigated and the results were discussed in detail.

2. Experimental

2.1. Materials

All reagents were of analytical grade and used without further purification. Double-distilled water was used throughout this study.

2.2. Instruments

The XRD patterns were recorded by a Philips Xpert X-ray diffractometer with Cu Kα radiation (λ = 0.15406 nm), employing scanning rate of 0.04˚/sec in the 2θ range from 20˚ to 80˚. Surface morphology and distribution of particles were studied by LEO 1430VP SEM, using an accelerating voltage of 15 kV. The purity and elemental analysis of the products were obtained by EDX on the same SEM instrument. The DRS was recorded by a Scinco 4100 apparatus. The PL spectra of the samples were studied using a Perkin Elmer (LS 55) fluorescence spectrophotometer with an excitation wavelength of 300 nm. The UV–vis spectra for the degradation reaction were studied using a Cecile 9000 spectrophotometer. A domestic microwave oven (2.45 GHz and 1,000 W) was used for preparation of the samples. The pH of solutions was measured using a Metrohm digital pH meter of model 691.

2.3. Preparation of ZnO/AgI nanocomposites

Typically for preparation of the nanocomposite with 0.188 mol fraction of silver iodide, 0.578 g of zinc nitrate tetrahydrate and 0.086 g of silver nitrate were dissolved in 100 mL of water under stirring at room temperature. Then, an aqueous solution of NaOH (5 M) was dropwise added to the solution under stirring at room temperature until pH of the solution reached 9.5. Afterward, an aqueous solution of sodium iodide (0.076 g dissolved in 50 mL of water) was slowly added to the formed light brown suspension. Then, the yellow suspension was irradiated in air for 15 min with 55% of output. The formed olive color product was centrifuged to get the precipitate out and washed twice with double-distilled water and ethanol to remove the unreacted reagents and dried in an oven at 60˚C for 24 h. The schematic diagram for preparation of the nanocomposites can be illustrated in Fig. 1.

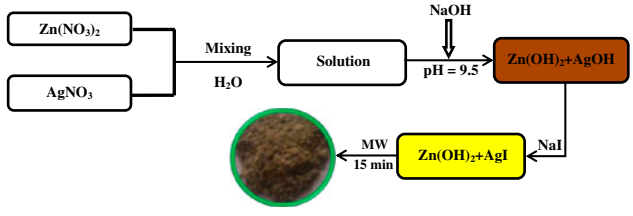

Fig. 1. The schematic diagram for preparation of ZnO/AgI nanocomposites using a simple one-pot microwave-assisted method.

2.4. Photocatalysis experiments

Photocatalysis experiments were performed in a cylindrical Pyrex reactor with about 400 mL capacity. Temperature of the reactor was maintained at 25°C using a water circulation arrangement. The solution was mechanically stirred and continuously aerated by a pump to provide oxygen and complete mixing of the reaction solution. An LED source with 50 W was used as a visible-light source. The emission spectrum of the source has high intensity in the visible range and its intensity rapidly decreases in wavelengths near to UV and IR ranges [29]. The source was fitted on the top of the reactor. Prior to illumination, a suspension containing 0.1 g of the photocatalyst and 250 mL of RhB solution (1×10^{-5} M) was continuously stirred in the dark for 60 min, to attain adsorption equilibrium. Samples were taken from the reactor at regular intervals and the photocatalyst removed before analysis by the spectrophotometer at 553 nm corresponding to the maximum absorption wavelength of RhB.

3. Results and discussion

Fig. 2(a) shows the XRD patterns for ZnO/AgI nanocomposites with different compositions. The pure ZnO and AgI samples have diffraction peaks ascribed to the wurtzite hexagonal (JCPDS 65-3411) and β phases of AgI (JCPDS 09-0374), respectively [30–32]. For the ZnO/AgI nanocomposites, the diffraction peaks are simply indexed to ZnO and AgI. Consequently, the diffraction patterns confirmed coexistence of ZnO and AgI in the nanocomposites.

Purity of the as-prepared samples was confirmed by EDX technique and the results for the ZnO nanostructures, AgI nanoparticles, and ZnO/AgI nanocomposite with 0.342 mol fraction of silver iodide are shown in Fig. 2(b). For the ZnO nanostructures, the peaks correspond to Zn and O elements. In the case of AgI nanoparticles, the peaks are simply related to Ag and I elements. For the nanocomposite, the peaks are assigned to Zn, O, Ag, and I elements. In this figure, the other peaks are corresponding to the elements applied for the sputter coating of the samples on the EDX stage.

Fig. 3 shows the SEM images for surface morphology of the as-prepared samples. For the ZnO nanostructures, they consist of highly aggregated oval-like particles. The silver iodide nanoparticles are formed by aggregation of nearly spherical particles with different sizes. In the case of the nanocomposites, the surface morphology is considerably changed with increasing mole fraction of AgI. As stated in the preparation section, particles of ZnO are formed in

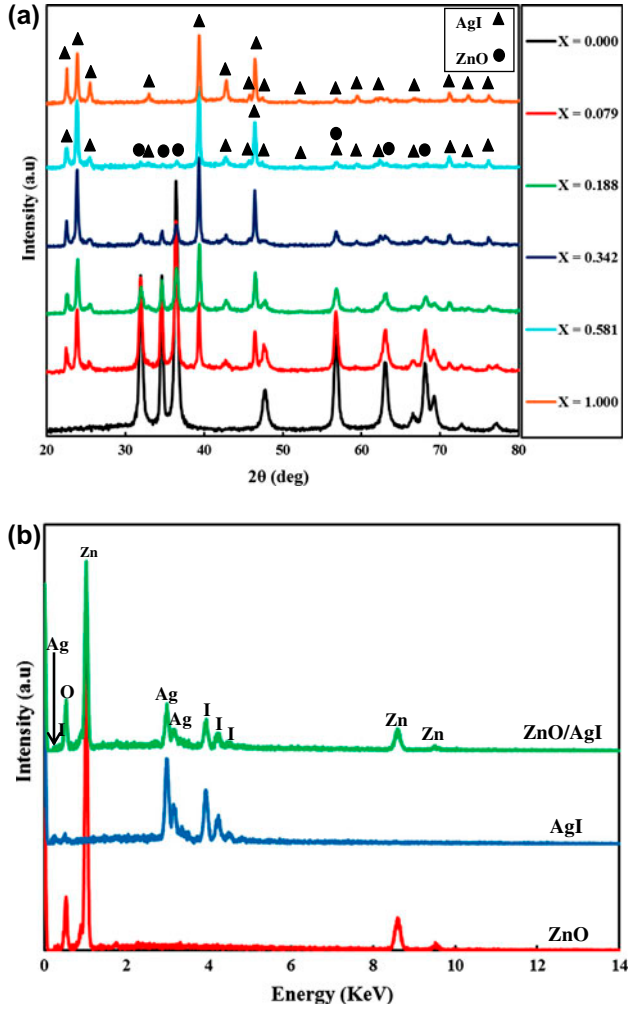

Fig. 2. (a) The XRD patterns for ZnO/AgI nanocomposites with various mole fractions of AgI and (b) The EDX spectra for ZnO, AgI, and the nanocomposite with 0.342 mol fraction of AgI.

presence of silver ions. In this reaction system, silver cations interact with oxygen moieties of ZnO, leading to control the size and shape of the nanocomposite.

It is well known that electronic properties of semiconductors could considerably affect their photocatalytic activities. Hence, the electronic properties of the samples were examined using UV–vis DRS technique and the results are shown in Fig. 4. The ZnO nanostructures show a strong absorption at 355 nm. Hence, there is a blue shift of 29 nm relative to the bulk ZnO due to quantum confinement effect [33]. In the case of the nanocomposites, it is evident that not only the absorption efficiency in the visible range was gradually enhanced with increasing mole fraction of silver iodide, but also the absorption edge was red shifted, leading to absorb more photons from the visible range

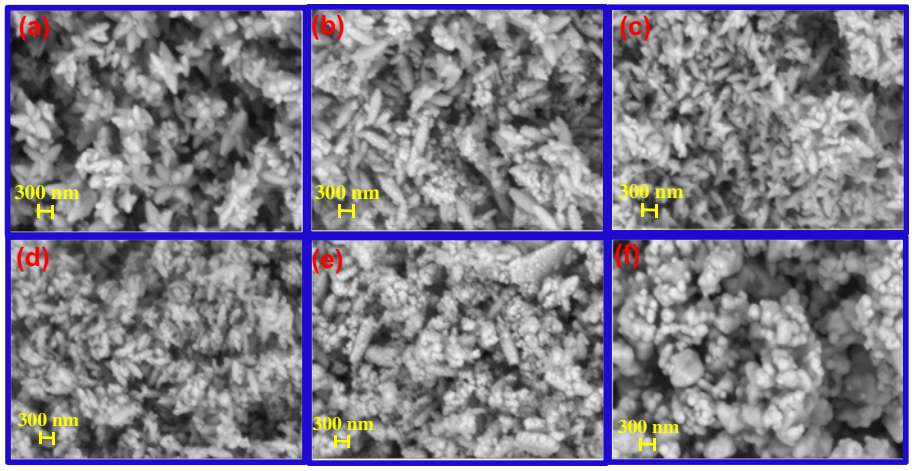

Fig. 3. The SEM images for ZnO/AgI nanocomposites with various mole fractions of AgI: (a) $X = 0$, (b) $X = 0.079$, (c) $X = 0.188$, (d) $X = 0.342$, (e) $X = 0.581$, and (f) $X = 1.000$.

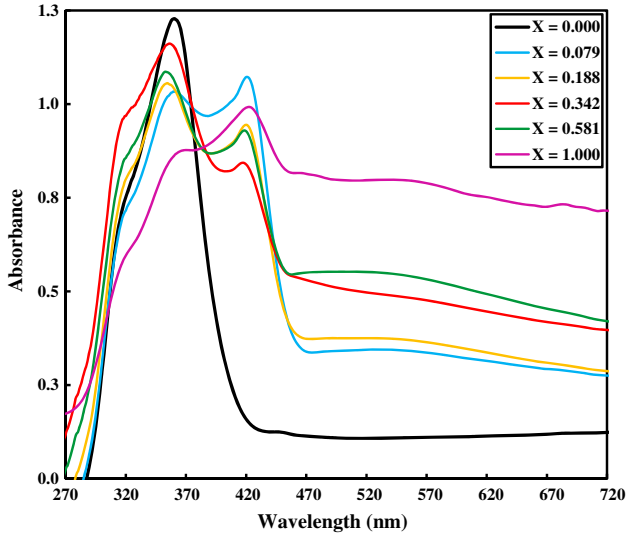

Fig. 4. The UV–vis DRS for ZnO/AgI nanocomposites with different mole fractions of AgI.

to produce more electron–hole pairs. As a result, it can be concluded that the nanocomposites could have noticeable activity under the visible-light irradiation.

Photocatalytic activity of the samples was investigated by degradation of RhB, as an organic pollutant, under the visible-light irradiation. Fig. 5(a) and (b) show plots of the absorbance vs. wavelength for the degradation of RhB over the ZnO nanostructures and the nanocomposite with 0.342 mol fraction of silver iodide under visible-light irradiation, respectively ([RhB] = 1×10^{-5} M, and catalyst weight = 0.1 g). It is evident that the degradation reaction on the nanocomposite takes place with higher rate than that of the ZnO nanostructures. In order to obtain optimum content of silver iodide in the nanocomposites, degradation of RhB over the prepared samples was carried out and the results are shown in Fig. 6(a). It is clear that mole fraction of silver iodide considerably influences on the degradation reaction and the best activity was seen for the nanocomposite with 0.342 mol fraction of AgI. After the light irradiation for 405 min, about 14 and 97% of RhB were degraded over the ZnO nanostructures and the nanocomposite, respectively. The degradation rate constants for different samples were calculated [16] and the results are shown in Fig. 6(b). As can be seen, the rate constant increases with increasing mole fraction of silver iodide up to 0.342 and then decreases. The degradation rate constant on the ZnO nanostructures and the nanocomposite are 7.40×10^{-4}–78.0×10^{-4} min^{-1}, respectively. Therefore, activity of the nanocomposite has enhanced about 10-fold relative to the ZnO nanostructures.

Compared to the ZnO nanostructures, the enhancing photocatalytic activity of the nanocomposites may be related to decrease the recombination of electron–hole pairs. In order to confirm this, the PL spectra of the ZnO nanostructures and the nanocomposite with 0.342 mol fraction of silver iodide were provided (Fig. 7). Generally, a higher PL intensity indicates a higher recombination of the electron–hole pairs [34]. It is clearly evident that the PL intensity for the nanocomposite is lower than that of the ZnO nanostructures. Hence, it was concluded that the separation of the charge carriers in the nanocomposite is higher than that of the ZnO nanostructures. Consequently, due to decreasing recombination of the charge carriers, there will be more electron–hole pairs for

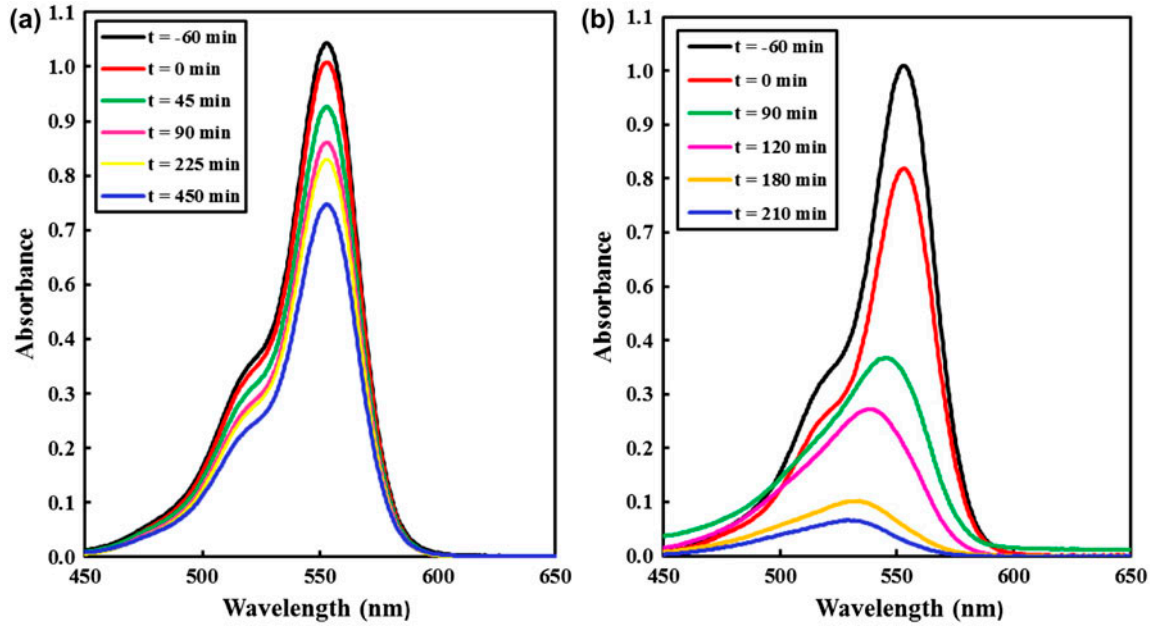

Fig. 5. The UV–vis spectra for degradation of RhB under visible-light irradiation over: (a) the ZnO nanostructures and (b) ZnO/AgI nanocomposite with 0.342 mol fraction of AgI ([RhB] = 1×10^{-5} M, photocatalyst weight = 0.1 g).

participating in the degradation reactions and as a result, the degradation reaction is enhanced compared to the bare ZnO. A possible mechanism for increasing photocatalytic activity of the ZnO/AgI nanocomposites under visible-light irradiation relative to that of the ZnO is proposed (Fig. 8). When the nanocomposite is illuminated by the visible light, only AgI is excited and the electrons in its valence band (VB) are excited to the conduction band (CB) and the same number of holes is left in the VB; because band gap of AgI (2.80 eV) is lower than that of the ZnO (3.20 eV) [19–21]. The VB and CB energies of AgI calculated based on Butler and Ginley model are −0.42 and +2.37 eV and those for ZnO are −0.34 and +2.86 eV, respectively [35]. After that, the photo-induced electrons are easily injected from the CB of AgI to that of the ZnO, because the CB of AgI is more negative than that of the ZnO. The potential of $O_2/\cdot O_2^-$ (−0.33 eV) is less negative than CB of the ZnO. Hence, over the ZnO, oxygen molecules are easily changed to $\cdot O_2^-$ [36]. After that, the produced $\cdot O_2^-$ ions react with the dye molecules to produce the degradation products. Furthermore, the potential for O_2/H_2O_2 (+0.695 eV) is more positive than the CB energy of ZnO. Hence, the electrons in CB of ZnO react with adsorbed oxygen to produce H_2O_2. The produced hydrogen peroxide molecules subsequently generates ·OH radicals by capturing electrons [37]. Therefore, the photo-generated electrons transfer from the CB of AgI to that of ZnO and holes remain on VB of AgI, leading to separation and increasing lifetime of the charge carriers to participate in the degradation reactions. As a result, the activity of the nanocomposites increased relative to that of the ZnO. It is noteworthy that oxidation of the adsorbed $^-$OH and H_2O to hydroxyl radicals does not take place on the VB of AgI because the potential for VB of AgI (+2.37 eV) is not enough for oxidation of adsorbed $^-$OH ($E^\circ_{^-OH/OH^\circ}$ = +2.38 eV) and H_2O ($E^\circ_{H_2O/OH^\circ}$ = +2.72 eV) [38]. Hence, the holes on VB of AgI react directly with adsorbed molecules of RhB to produce the degradation products. The role of these reactive species in degradation of RhB on the nanocomposite was examined using a series of scavengers. Fig. 9 shows a plot of the rate constant for degradation of RhB on the nanocomposite in the presence of the selected scavengers. As can be seen, decrease in the rate constant in the presence of benzoquinone (scavenger for $\cdot O_2^-$) is higher than those of 2-PrOH (scavenger for ·OH) and ammonium oxalate (scavenger for holes). Hence, it is concluded that superoxide ions play a key role in degradation of RhB on the nanocomposites.

It is well known that preparation time and calcination temperature remarkably affect crystallinity, size, and morphology of nanomaterials; hence, these parameters can affect photocatalytic activity [29,39]. In order to investigate the influence of the microwave irradiation time, six comparative samples were

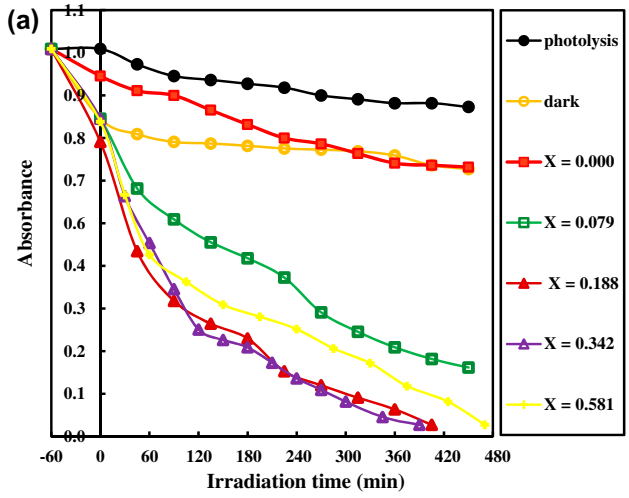

Fig. 6. (a) Photodegradation of RhB over ZnO/AgI nanocomposites with different mole fraction of AgI along with photolysis and dark data and (b) Plot of the degradation rate constant of RhB over the samples with different mole fractions of AgI under visible-light irradiation.

prepared by the irradiations for 3, 6, 9, 12, 15, and 20 min and the results are shown in Fig. 10(a). It is clear that the best activity is seen for the nanocomposite prepared by microwave irradiation for 15 min. Therefore, this nanocomposite was selected for further experiments. To investigate the effect of calcination temperature on the photocatalytic activity, the nanocomposite was calcined for 2 h at 200, 300, 400, and 500°C and the results are depicted in Fig. 7(b). As can be seen, degradation of RhB over the nanocomposite without any thermal treatment is faster than those of the calcined samples. Photocatalytic activity is usually related to surface area and other textural properties of photocatalysts [1,4]. With increase in the calcination temperature, size, and aggregation of

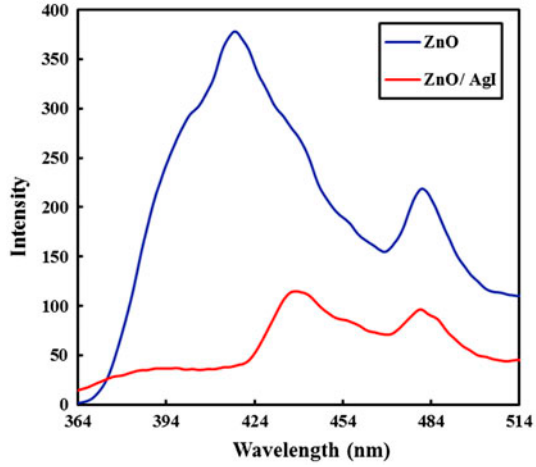

Fig. 7. The PL spectra for the ZnO nanostructures and the nanocomposite with 0.342 mol fraction of AgI.

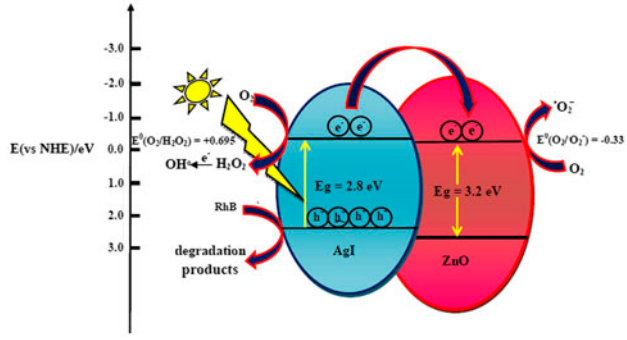

Fig. 8. The possible mechanism for degradation of RhB over the ZnO/AgI nanocomposites.

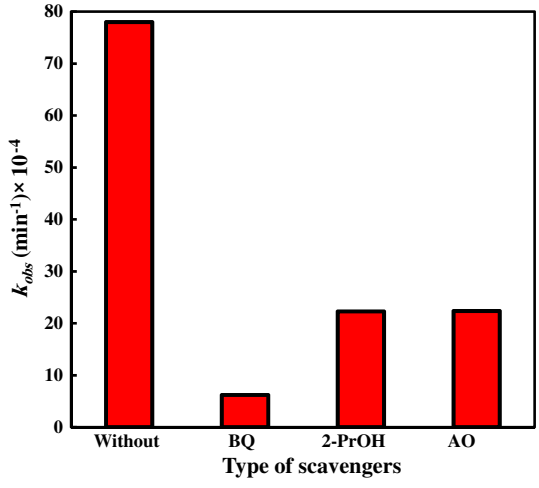

Fig. 9. The degradation rate constant of RhB over the nanocomposite with 0.342 mol fraction of AgI in presence of various scavengers.

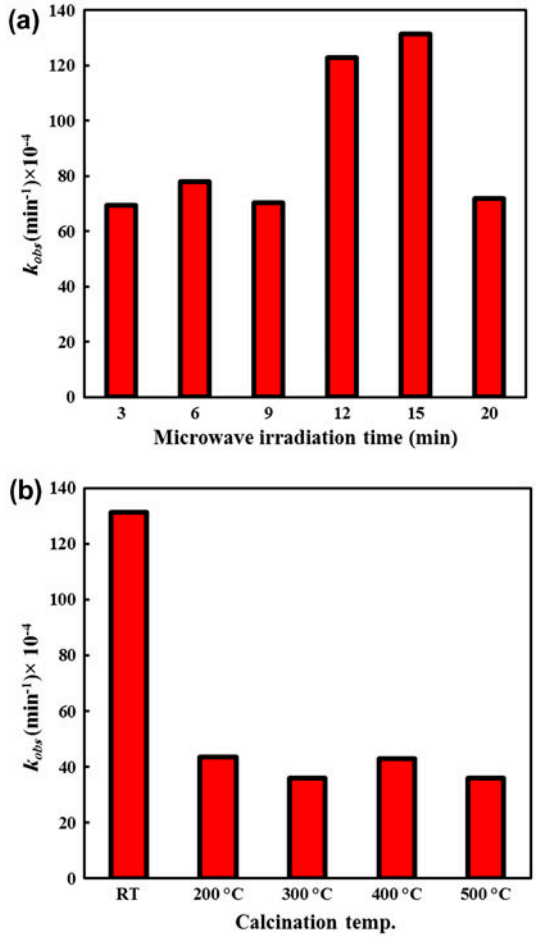

Fig. 10. (a) The degradation rate constant of RhB over the nanocomposite with 0.342 mol fraction of AgI prepared at different microwave irradiation times and (b) The degradation rate constant of RhB on the nanocomposite calcined at different temperatures.

photocatalysts are increased, leading to decrease in their surface area and pore volume [39]. Hence, decrease in the photocatalytic activity can be related to increase in size and aggregation of particles at higher temperatures [29,39].

It is well known that besides photocatalytic activity, stability of photocatalysts is very important for their practical applications. In order to know reusability of the nanocomposite, the degradation experiments were carried out and the results are demonstrated in Fig. 11. As can be seen, the degradation percent decreases to about 80% after five runs. Hence, the photocatalyst has good stability and reusability. Decrease in the degradation efficiency can be related to photocorrosion of the photocatalyst under the light irradiation [12].

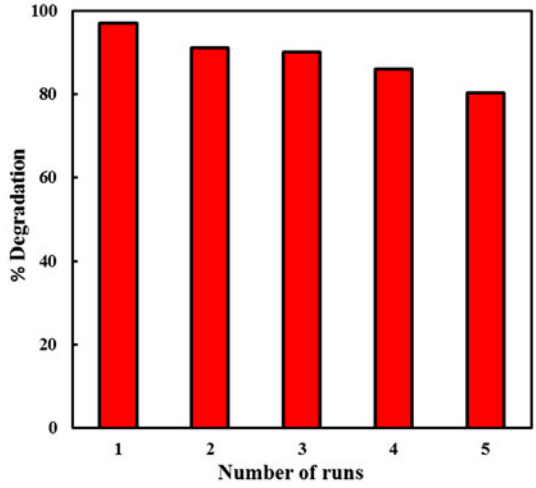

Fig. 11. Reusability of the nanocomposite after five successive runs.

4. Conclusion

In summary, we successfully prepared ZnO/AgI nanocomposites as visible-light-driven photocatalysts by a simple one-pot microwave-assisted method, for the first time. The as-prepared samples were characterized using XRD, EDX, SEM, DRS, and PL techniques. Photocatalytic activity of the samples was investigated by degradation of rhodamine B under visible-light irradiation. Activity of the nanocomposites was gradually enhanced with increasing mole fraction of silver iodide and the superior activity was seen for 0.342 mol fraction of AgI. The degradation rate constant over this nanocomposite is about 10-fold greater than that of the ZnO nanostructures. Based on the results obtained from DRS and PL techniques, enhancing photocatalytic activity of the nanocomposites was attributed to their ability for more absorption in the visible range and effectively separation of the charge carriers. The nanocomposite prepared by microwave irradiation for 15 min has the highest activity relative to the other preparation times. Furthermore, the degradation reaction on the nanocomposite without any thermal treatment is faster than those of the calcined samples. Finally, the photocatalyst has a good stability and retains about 80% of its activity after using for five cycles.

Acknowledgment

The authors wish to acknowledge University of Mohaghegh Ardabili, for financial support of this work.

References

[1] C.C. Chen, W.H. Ma, J.C. Zhao, Semiconductor-mediated photodegradation of pollutants under visible-light irradiation, Chem. Soc. Rev. 39 (2010) 4206–4219.

[2] K. Li, X. An, K.H. Park, M. Khraisheh, J. Tang, A critical review of CO_2 photoconversion: Catalysis and reactors, Catal. Today 224 (2014) 3–12.

[3] H. Ahmad, S.K. Kamarudin, L.J. Minggu, M. Kassim, Hydrogen from photocatalytic water splitting process: A review, Renewable Sustainable Energy Rev. 43 (2015) 599–610.

[4] B. Ohtani, Photocatalysis A to Z—What we know and what we do not know in a scientific sense, J. Photochem. Photobiol. C: Photochem. Rev. 11 (2010) 157–178.

[5] B. Li, Y. Wang, Synthesis, microstructure, and photocatalysis of ZnO/CdS nano-heterostructure, J. Phys. Chem. Solids 72 (2011) 1165–1169.

[6] B. Li, T. Liu, Y. Wang, Z. Wang, ZnO/graphene-oxide nanocomposite with remarkably enhanced visible-light-driven photocatalytic performance, J. Colloid Interface Sci. 377 (2012) 114–121.

[7] Y. Wang, Q. Wang, X. Zhan, F. Wang, M. Safdar, J. He, Visible-light-driven type II heterostructures and their enhanced photocatalysis properties: A review, Nanoscale 5 (2013) 8326–8339.

[8] F. Yang, B. Tian, J. Zhang, T. Xiong, T. Wang, Preparation, characterization, and photocatalytic activity of porous AgBr@Ag and AgBrI@Ag plasmonic photocatalysts, Appl. Surf. Sci. 292 (2014) 256–261.

[9] Z.-M. Yang, Y. Tian, G.-F. Huang, W.-Q. Huang, Y.-Y. Liu, C. Jiao, Z. Wan, X.-G. Yan, A. Pan, Novel 3D flower-like Ag_3PO_4 microspheres with highly enhanced visible light photocatalytic activity, Mater. Lett. 116 (2014) 209–211.

[10] Y. Song, J. Zhu, H. Xu, C. Wang, Y. Xu, H. Ji, K. Wang, Q. Zhang, H. Li, Synthesis, characterization and visible-light photocatalytic performance of Ag_2CO_3 modified by graphene-oxide, J. Alloys Compd. 592 (2014) 258–265.

[11] F. Soofivand, F. Mohandes, M. Salavati-Niasari, Silver chromate and silver dichromate nanostructures: Sonochemical synthesis, characterization, and photocatalytic properties, Mater. Res. Bull. 48 (2013) 2084–2094.

[12] S. Naghizadeh-Alamdari, A. Habibi-Yangjeh, M. Pirhashemi, One-pot ultrasonic-assisted method for preparation of Ag/AgCl sensitized ZnO nanostructures as visible-light-driven photocatalysts, Solid State Sci. 40 (2015) 111–120.

[13] B. Krishnakumar, B. Subash, M. Swaminathan, AgBr–ZnO—An efficient nano-photocatalyst for the mineralization of Acid Black 1 with UV light, Sep. Purif. Technol. 85 (2012) 35–44.

[14] C. Wu, L. Shen, Y.C. Zhang, Q. Huang, Synthesis of AgBr-ZnO nanocomposite with visible light-driven photocatalytic activity, Mater. Lett. 66 (2012) 83–85.

[15] M. Alan, Q. YanYan, Z. LiNa, X. Xiao, L. ZhenJiang, Sunlight responsive photocatalysts: AgBr/ZnO hybrid nanomaterial, Sci. China Chem. 55 (2012) 2128–2133.

[16] M. Pirhashemi, A. Habibi-Yangjeh, Simple and large scale one-pot method for preparation of AgBr–ZnO nanocomposites as highly efficient visible light photocatalyst, Appl. Surf. Sci. 283 (2013) 1080–1088.

[17] L. Shi, L. Liang, J. Ma, J. Sun, Improved photocatalytic performance over AgBr/ZnO under visible light, Superlattices Microstruct. 62 (2013) 128–139.

[18] C. Dong, K.-L. Wu, M.-R. Li, L. Liu, X.-W. Wei, Synthesis of Ag_3PO_4–ZnO nanorod composites with high visible-light photocatalytic activity, Catal. Commun. 46 (2014) 32–35.

[19] K. Vignesh, A. Suganthi, M. Rajarajan, S.A. Sara, Photocatalytic activity of AgI sensitized ZnO nanoparticles under visible light irradiation, Powder Technol. 224 (2012) 331–337.

[20] J. Lu, H. Wang, Y. Dong, F. Wang, S. Dong, Plasmonic AgX nanoparticles-modified ZnO nanorod arrays and their visible-light-driven photocatalytic activity, Chin. J. Catal. 35 (2014) 1113–1125.

[21] X. Wang, X. Wan, X. Xu, X. Chen, Facile fabrication of highly efficient AgI/ZnO heterojunction and its application of methylene blue and rhodamine B solutions degradation under natural sunlight, Appl. Surf. Sci. 321 (2014) 10–18.

[22] S. Shaker-Agjekandy, A. Habibi-Yangjeh, Facile one-pot method for preparation of AgI/ZnO nanocomposites as visible-light-driven photocatalysts with enhanced activities, Mater. Sci. Semicond. Process. 34 (2015) 74–81.

[23] M. Zhou, Y. Hu, Y. Liu, W. Yang, H. Qian, Microwave-assisted route to fabricate coaxial ZnO/C/CdS nanocables with enhanced visible light-driven photocatalytic activity, Cryst. Eng. Commun. 14 (2012) 7686–7693.

[24] Y. Liu, Y. Hu, M. Zhou, H. Qian, X. Hu, Microwave-assisted non-aqueous route to deposit well-dispersed ZnO nanocrystals on reduced graphene oxide sheets with improved photoactivity for the decolorization of dyes under visible light, Appl. Catal., B: Environ. 125 (2012) 425– 431.

[25] L. Li, X. Zhang, W. Zhang, L. Wang, X. Chen, Y. Gao, Microwave-assisted synthesis of nanocomposite Ag/ZnO–TiO_2 and photocatalytic degradation Rhodamine B with different modes, Colloids Surf., A: Physicochem. Eng. Aspects 457 (2014) 134–141.

[26] L. Li, X. Huang, Y. Gao, W. Zhang, X. Zhang, X. Chen, Microwave-assisted synthesis of a series of Ag/ZnO nanocomposites and evaluation of their photocatalytic activities under multi-mode photodegradation, Aust. J. Chem. 68 (2015) 774–782.

[27] J. He, J. Wang, Y. Liu, Z.A. Mirza, C. Zhao, W. Xiao, Microwave-assisted synthesis of BiOCl and its adsorption and photocatalytic activity, Ceram. Int. 41 (2015) 8028–8033.

[28] B. Baruwati, V. Polshettiwar, R.S. Varma, Microwave-assisted synthesis of nanomaterials in aqueous media, in: V. Polshettiwar, R.S. Varma (Eds.), Aqueous microwave assisted chemistry, synthesis and catalysis, RSC, Cambridge, pp. 176–209.

[29] M. Shekofteh-Gohari, A. Habibi-Yangjeh, Facile preparation of Fe_3O_4@AgBr–ZnO nanocomposites as novel magnetically separable visible-light-driven photocatalysts, Ceram. Int. 141 (2015) 1467–1476.

[30] B.G. Mishra, G.R. Rao, Promoting effect of ceria on the physicochemical and catalytic properties of CeO_2–ZnO composite oxide catalysts, J. Mol. Catal. A: Chem. 243 (2006) 204–213.

[31] H. Xu, J. Yan, Y. Xu, Y. Song, H. Li, J. Xia, C. Huang, H. Wan, Novel visible-light-driven AgX/graphite-like C_3N_4 (X = Br, I) hybrid materials with synergistic photocatalytic activity, Appl. Catal. B: Environ. 129 (2013) 182– 193.
[32] F. Mohandes, M. Salavati-Niasari, Application of a new coordination compound for the preparation of AgI nanoparticles, Mater. Res. Bull. 48 (2013) 3773–3782.
[33] X.-H. Guo, J.-Q. Ma, H.-G. Ge, Preparation, characterization, and photocatalytic performance of pear-shaped ZnO/Ag core-shell submicrospheres, J. Phys. Chem. Solids 74 (2013) 784–788.
[34] S. Wang, D. Li, C. Sun, S. Yang, Y. Guan, H. He, Synthesis and characterization of g-C_3N_4/Ag_3VO_4 composites with significantly enhanced visible-light photocatalytic activity for triphenylmethane dye degradation, Appl. Catal. B: Environ. 144 (2014) 885–892.
[35] S.R. Morrison, Electrochemistry at Semiconductor and Oxidized Metal Electrode, Plenum, New York, NY, 1980.
[36] J. Kim, C.W. Lee, W. Choi, Platinized WO_3 as an environmental photocatalyst that generates OH radicals under visible light, Environ. Sci. Technol. 44 (2010) 6849−6854.
[37] G. Li, K.H. Wong, X. Zhang, C. Hu, J.C. Yu, R.C.Y. Chan, P.K. Wong, Degradation of acid orange 7 using magnetic AgBr under visible light: The roles of oxidizing species, Chemosphere 76 (2009) 1185–1191.
[38] J. Jiang, H. Li, L.Z. Zhang, New insight into daylight photocatalysis of AgBr@Ag: synergistic effect between semiconductor photocatalysis and plasmonic photocatalysis, Chem. Eur. J. 18 (2012) 6360–6369.
[39] S.Y. Kim, T.H. Lim, T.S. Chang, C.H. Shin, Photocatalysis of methylene blue on titanium dioxide nanoparticles synthesized by modified sol-hydrothermal process of $TiCl_4$, Catal. Lett. 117 (2007) 112–118.